INTERNATIONAL JOURNAL OF RESEARCH IN MECHANICAL, MECHATRONICS AND AUTOMOBILE ENGINEERING(IJRMMAE)
ISSN: 2454-1435 (Print) | 2454-1443 (online)
Volume 6 Issue 4, January – March 2021 - www.ijrmmae.in – Pages 49-65

# CHARACTERIZATION OF DIAMOND LIKE CARBON (DLC) COATINGS BY PULSED MAGNETRON SPUTTERING FOR CUTTING TOOL APPLICATIONS

**Meenatchisundaram P, Gangadharan T, Ramachandran V, Saravanan S, ArunPrabhaharan M**

Department of Mechanical Engineering, Sethu Institute of Technology, Virudhunagar, India

**Received: 3rd December 2020 | Accepted: 10th February 2021**

**Abstract**

A shut field adjusted magnetron faltering framework is utilized to store Ti doped DLC covered on hardened steel plates and miniature drills. The microstructures of the different coatings are examined utilizing filtering electron magnifying instrument, while the coefficient of grinding is broke down utilizing block on ring wear analyzer. The penetrating presentation of the covered miniature drills is assessed by leading rapid through-opening boring tests utilizing Tempered steel plate examples. The help life of the covered miniature drills is evaluated using various standards, in particular surface harshness of the bored opening, and the wear of the front line, separately. In general, the outcomes show that the Ti doped DLC covering has the ideal fast machining execution, for example it broadens the device life by a variable of something like four contrasted with the uncoated miniature drill and yields a critical improvement in the machining quality.

**Keywords.** General Characterization, Nano structured Ti-DLC coating, Magnetron Sputtering.

## INTRODUCTION

A straightforward, quick, and non-destructive method for analyzing both organic and inorganic substances is Raman spectroscopy. Raman spectroscopy is a kind of molecular spectroscopy in which molecules or atoms scatter electromagnetic energy [14]. It gauges molecules' vibrational, rotational, and other low-frequency modes [12]. Raman spectroscopy has a number of benefits [11]. In actuality, transparent containers such as

INTERNATIONAL JOURNAL OF RESEARCH IN MECHANICAL, MECHATRONICS AND AUTOMOBILE ENGINEERING(IJRMMAE)
ISSN: 2454-1435 (Print) | 2454-1443 (online)
Volume 6 Issue 4, January – March 2021 - www.ijrmmae.in – Pages 49-65

glasses, jars, plastic bags, cuvettes, and others can be used directly for Raman analysis [3]. As an example, this method requires little sample preparation and is nondestructive.

Furthermore, both qualitative and quantitative examination can be done with Raman. Because of its high selectivity, this method makes it simple to distinguish between molecules in extremely similar compounds. Raman equipment is lightweight, portable, and easy to use [3]. Indeed, even a nontechnical client can play out the investigation and immediately get the information, in this way empowering specialists on call for embrace reasonable precautionary measures relying upon the kind of materials being looked through on the scene [9].

A typical procedure utilized for the majority covering processes, in which the high lively argon particles barrage the graphite cathodes to store DLC films [5]. Plasma is created by utilizing either a DC or RF power [5]. Unadulterated carbon plasma with a wide energy conveyance is delivered by the impingement of the fiery particles on the graphitic target. A mix of hydrogen or CH4 plasma with the Ar plasma results in hydrogenated DLC (a-C:H), while for it started DLC nitrogen replaces either hydrogen or Ar[5]. The disadvantages of this cycle, for example, low testimony rates, low particle efficiencies in the plasma and the high substrate warming impacts, can be overwhelmed by the magnetron faltering interaction [7]. Here the magnets put behind the objective builds the way length of the electrons by giving them a winding movement, in this manner expanding the level of ionization of the plasma and the resultant yield [7]. The lopsided magnetron and particle helped affidavit processes are the enhancements of the faltering strategies for getting high thickness films [8].

## 2. EXPERIMENTAL DETAIL

### 2.1 SUBSTRATE CLEANING PROCESS

.**CLEANING OF STAINLESS STEEL TOOL**; The most important phase in cleaning of hardened steel surface (15 × 15 mm) was to sonicate utilizing CH3)2CO. CH3)2CO eliminates oil and other dampness on the steel surface.

**2.2 COATING DEPOSITION** After substrate cleaning process, the coatings were stored on hardened steel circles and 1mm miniature drills utilizing a shut field adjusted magnetron faltering framework (Rear HIVAC, Bangalore) with a solitary Titanium target, single graphite target and CH4 as the receptive gas. In first cycle the DLC was kept on the circle and the boring apparatus. The second cycle Ti doped DLC was stored on another circle and boring apparatus. The circumstances for the testimony cycle are displayed in underneath.

| S. No. | Target material | Sputtering/ Reactive gas | Material | Chamber pressure | Power (W) | Substrate temperature |
|---|---|---|---|---|---|---|
| 1 | Graphite | Ar /$CH_4$ | SS plate & drill bits | 2x10-3 | 89 | RT |
| 2 | Ti/Graphite | Ar /$CH_4$ | Ss plate& drill bits | 3x10-3 | 90 | RT |

**Table 2.1 Experimental Detail**

## 3. CHARACTERIZATION TECHNIQUES

Raman spectroscopy is a profoundly flexible strategy that gives a straightforward, quick and non-horrendous investigation of both natural and inorganic synthetic substances. Raman spectroscopy is a sort of sub-atomic spectroscopy that includes the scattering of electromagnetic radiation by particles or molecules. It gauges the rotational, vibrational, and other low-recurrence methods of atoms.

Raman spectroscopy offers a few benefits. For example, this strategy is nondestructive and nearly nothing or test readiness. As a matter of fact, Raman examination can be led straightforwardly by means of glasses, containers, plastic packs, cuvettes, and other straightforward holders. In addition, Raman can be utilized for subjective as well as quantitative examination. This strategy is profoundly specific, and that implies that it can without much of a stretch separate particles in synthetics that are basically the same. Raman instrumentation is minimal, compact and easy to understand. Indeed, even a nontechnical client can play out the examination and immediately get the information, in this manner empowering specialists on call for take on reasonable precautionary measures relying upon the sort of materials being looked through on the scene. A Raman spectrometer incorporates three fundamental parts like the laser, the inspecting connection point, and the actual spectrometer. A commonplace Raman laser will comprises of various qualities, for example, a little structure factor, low power utilization, limited line width, a steady power yield, and a steady frequency yield. In the event that Raman estimations are directed utilizing a 785nm source, it is critical to guarantee that the source is just radiating 785nm.

The subsequent part incorporates the inspecting point of interaction. In numerous Raman spectrometers, fiber-optic test is normally utilized which offers a very adaptable examining connection point. These fiber-optic tests can be effortlessly adjusted to a scope of optical magnifying instruments, gas stream cells, fluid stream cells, and other examining chambers. One basic part of a fiber-optic test is a high-optical-thickness Raman cutoff. This implies, when clients are taking a gander at the Raman range, they need to guarantee that the laser frequency is impeded however much as could reasonably be expected so the Raman shift can be noticed. The Raman should move is noticed extremely near the laser line since numerous materials have crucial ghastly elements exceptionally close to the line.

The third part is the spectrometer. Here, significant execution factors are little structure factor, high goal, low power utilization, and low clamor. A proper indicator is vital and should be used relying upon which excitation laser is being utilized. For noticeable excitation, a standard CCD is chosen; for UV excitation, a photomultiplier tube (PMT) or CCD is commonly picked; and for NIR excitation, an indium gallium arsenide (InGaAs) cluster is regularly utilized.


**Figure 1 Transmission Microscope**

### 3.1 SEM ANALYSIS

A Filtering Electron Magnifying lens (SEM) is a kind of electron magnifying lens that produces pictures of an example by checking it with an engaged light emission. The electrons communicate with iotas in the example, delivering different signs that can be recognized and that contain data about the example's surface geography and composition. SEM can accomplish goal better than 1 nanometer. Examples can be seen in high vacuum, in low vacuum, and (in natural SEM) in wet circumstances.

### 3.1.1 SCANNING PROCESS &IMAGE FORMATION

At the highest point of the Fig 2 is the section where the electron shaft is produced and centered. From the section comes the electron bar, likewise called the essential electrons, displayed here as x-beam. At the point when the essential electrons influence the surface they produce auxiliary electrons, backscattered electrons, Drill electrons, X-beam photons and cathode iridescence.  The electron bar, which regularly has an energy going from 0.2 keV to 40 keV, is engaged by a couple of condenser focal points to a spot around 0.4 nm to 5 nm in measurement. The pillar goes through sets of examining loops or sets of redirector plates in the electron section, commonly in the last focal point, which divert the bar in the x and y tomahawks so it checks in a raster style over a rectangular region of the example surface.

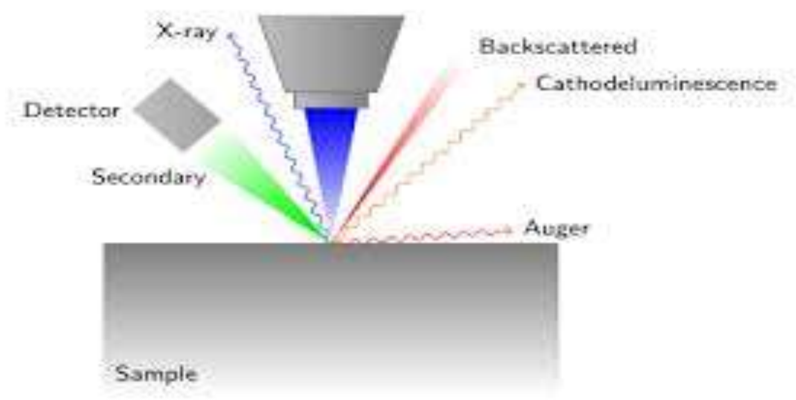


**Figure 2 Mechanism of Scanning Electron Microscope.**

At the point when the essential electron shaft communicates with the example, the electrons lose energy by rehashed irregular dissipating and ingestion inside a tear formed

INTERNATIONAL JOURNAL OF RESEARCH IN MECHANICAL, MECHATRONICS AND AUTOMOBILE ENGINEERING(IJRMMAE)
ISSN: 2454-1435 (Print) | 2454-1443 (online)
Volume 6 Issue 4, January – March 2021 - www.ijrmmae.in – Pages 49-65

volume of the example known as the collaboration volume, which stretches out from under 100 nm to roughly 5 µm into the surface. The size of the connection volume relies upon the electron's arrival energy, the nuclear number of the example and the example's thickness. The energy trade between the electron shaft and the example brings about the impression of high-energy electrons by versatile dissipating, outflow of auxiliary electrons by inelastic dispersing and the emanation of electromagnetic radiation, every one of which can be recognized by specific identifiers. The bar current consumed by the example can likewise be identified and used to make pictures of the dissemination of example current. Electronic speakers of different kinds are utilized to enhance the signs, which are shown as varieties in splendor on a PC screen (or, for rare models, on a cathode beam tube). Every pixel of PC video memory is synchronized with the place of the bar on the example in the magnifying lens, and the subsequent picture is in this manner a circulation guide of the power of the sign being radiated from the filtered region of the example. In more established magnifying lens picture might be caught by photography from a high-goal cathode beam tube, however in present day machines picture is saved to PC information capacity.

**3.1.2 DETECTION OF SECONDARY ELECTRONS**

The most well-known imaging mode gathers low-energy (<50 eV) optional electrons that are catapulted from the k-shell of the example molecules by inelastic dissipating cooperation’s with bar electrons. Because of their low energy, these electrons begin inside a couple of nanometers from the example surface. The electrons are identified by an Everhart-Thorley locator, which is a kind of scintillator-photomultiplier framework. The optional electrons are first gathered by drawing in them towards an electrically one-sided matrix at about +400 V, and afterward further advanced towards a phosphor or shine decidedly one-sided to about +2,000 V. The sped up optional electrons are presently adequately lively to cause the shine to produce blazes of light (cathode glow), which are directed to a photomultiplier outside the SEM section through a light line and a window in the mass of the example chamber. The enhanced electrical sign result by the photomultiplier is shown as a two-layered power conveyance that can be seen and captured on a simple video show, or exposed to simple to-computerized transformation and showed and saved as a computerized picture. This cycle depends on a raster-examined essential bar. The splendor of the sign relies upon the quantity of optional electrons arriving at the indicator. On the off chance that the bar enters the example opposite to the surface, the enacted locale is uniform about the hub of the pillar and a specific number of electrons "escape" from inside the example. As the point of frequency expands, the "escape" distance of one side of the bar will diminish, and more optional electrons will be radiated. In this way steep surfaces and edges will generally be more brilliant than level surfaces, which brings about pictures with a clear cut, three-layered appearance. Utilizing the sign of optional electrons picture goal under 0.5 nm is conceivable.

### 3.1.3 DETECTION OF BACKSCATTERED ELECTRONS

Backscattered electrons (BSE) comprise of high-energy electrons starting in the electron pillar that are reflected or back-dispersed out of the example communication volume by versatile dissipating collaborations with example particles. Since weighty components (high nuclear number) backscatter electrons more unequivocally than light components (low nuclear number), and hence seem more brilliant in the picture, BSE are utilized to distinguish balance between regions with various substance arrangements. The Everhart-Thornley finder, which is ordinarily situated aside of the example, is wasteful for the identification of backscattered electrons since few such electrons are transmitted in the strong point subtended by the locator, and on the grounds that the emphatically one-sided recognition framework has little capacity to draw in the higher energy BSE. Devoted backscattered electron locators are situated over the example in a "donut" type plan, concentric with the electron shaft, boosting the strong point of assortment. BSE identifiers are typically both of scintillator and of semiconductor types. At the point when all pieces of the identifier are utilized to gather electrons evenly about the shaft, nuclear number differentiation is created. Nonetheless, solid geographical differentiation is created by gathering back-dissipated electrons from one side over the example utilizing a lopsided, directional BSE indicator; the subsequent difference shows up as light of the geography from that side. Semiconductor finders can be made in spiral fragments that can be exchanged in or out to control the kind of difference delivered and its directionality. Backscattered electrons can likewise be utilized to shape electron backscatter diffraction (EBSD) picture that can be utilized to decide the crystallographic construction of the example.

### 3.1.4 RESOLUTION OF SEM

The spatial goal of the SEM relies upon the size of the electron spot, which thus relies upon both the frequency of the electrons and the electron-optical framework that delivers the checking bar. The goal is likewise restricted by the size of the communication volume, or the degree to which the material connects with the electron shaft. The spot size and the communication volume are both enormous contrasted with the distances between molecules, so the goal of the SEM isn't sufficiently high to picture individual iotas, as is conceivable in the more limited frequency (for example higher energy) transmission electron magnifying lens (TEM). The SEM has repaying benefits, however, including the capacity to picture a nearly huge region of the example; the capacity to picture mass materials (not simply meager movies or foils); and the range of scientific modes accessible for estimating the piece and properties of the example. Contingent upon the instrument, the goal can fall somewhere close to under 1 nm and 20 nm. By 2009, the world's most elevated SEM goal at high-bar energies (0.4 nm at 30 kV) is gotten with the Hitachi SU-9000.

## 3.2 AFM ANALYSIS

The AFM is one of the principal devices for imaging, estimating, and controlling matter at the nanoscale. The data is accumulated by "feeling" the surface with a mechanical test. Piezoelectric components that work with minuscule however exact and exact developments on (electronic) order empower the exceptionally exact filtering. In certain varieties, electric possibilities can likewise be filtered utilizing directing cantilevers.

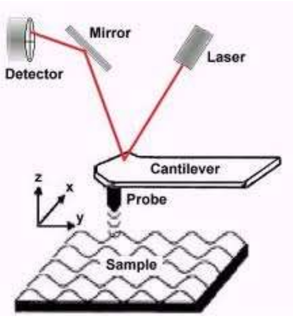


**Fig 3 schematic diagram of Atomic Force Microscope**

## 4.1MODES OF OPERATIONS

### 4.2.1 CONTACT MODE

In contact mode, the tip is "hauled" across the outer layer of the example and the forms of the surface are estimated either utilizing the diversion of the cantilever straightforwardly or, all the more normally, utilizing the criticism signal expected to keep the cantilever at a consistent position. Since the estimation of a static sign is inclined to clamor and float, low solidness cantilevers are utilized to help the redirection signal. Near the outer layer of the example, alluring powers can be areas of strength for very, the tip to "snap-in" to the surface. Subsequently, contact mode AFM is quite often finished at a profundity where the general power is terrible, that is to say, in firm "contact" with the strong surface underneath any adsorbed layers.

**4.2.2 TAPPING MODE**

In tapping mode, the cantilever is headed to waver all over at close to its reverberation recurrence by a little piezoelectric component mounted in the AFM tip holder like non-contact mode. Be that as it may, the sufficiency of this wavering is more noteworthy than 10 nm, normally 100 to 200 nm. The collaboration of powers following up on the cantilever when the tip comes near the surface, Van der Waals powers, dipole communications, electrostatic powers, and so on make the adequacy of this wavering lessening as the tip draws nearer to the example. An electronic servo purposes the piezoelectric actuator to control the level of the cantilever over the example. The servo changes the level to keep a set cantilever wavering sufficiency as the cantilever is looked over the example. An AFM picture is hence created by imaging the power of the irregular contacts of the tip with the example surface.

This strategy for "tapping" decreases the harm done to the surface and the tip contrasted with the sum done in contact mode. Tapping mode is delicate enough in any event, for the perception of upheld lipid bilayers or adsorbed single polymer atoms under fluid medium.

**4.2.3 NON-CONTACT MODE**

In this mode, the tip of the cantilever doesn't contact the example surface. The cantilever is rather wavered at either its resounding recurrence (recurrence tweak) or simply above (plentifulness balance) where the sufficiency of swaying is commonly a couple of nanometers (<10 nm) down to a couple of picometers. The van der Waals powers, which are most grounded from 1 nm to 10 nm over the surface, or whatever other long-range force that reaches out over the surface demonstrations to diminish the reverberation recurrence of the cantilever. This lessening in full recurrence joined with the criticism circle framework keeps a consistent wavering sufficiency or recurrence by changing the normal tip-to-test distance. Estimating the tip-to-test distance at each (x,y) information point permits the filtering programming to develop a geographical picture of the example surface.

Non-contact mode AFM doesn't experience the ill effects of tip or test debasement impacts that are now and again saw subsequent to taking various outputs with contact AFM.

AFM used to concentrate on a superficial level morphology boundaries, for example, Root Mean Square (RMS) harshness, Number juggling normal unpleasantness and greatest pinnacle level harshness, etc.

$$\text{Root Mean Square Roughness } Rq=\sqrt{1/n}[\sum_{i=1}^{n} yi^{2}]$$

$$\text{Arithmetic average Roughness } Ra=1/n[\sum_{i=1}^{n} yi]$$

Maximum Peak Height Rp= max $y_i$

### 4.3Block on ring Test Method:

This test technique covers the strategy for deciding sliding wear of different materials utilizing the block-on-ring geometry. A stationary block example is squeezed with a steady power against a pivoting ring example at 90º to the ring's hub of revolution. Contact between the sliding surfaces of the block and ring brings about loss of material from the two pieces. Numerous materials can be created into blocks and rings, however the standard's accentuation is on metals. The test might be run at the heaps, speeds, and temperatures which reenact the help conditions with different greases and fluid.

## 5. RESULT AND DISCUSSION

In this part make sense of the outcome and conversation for the Raman examination, SEM and AFM investigation, and coefficient of grating and Subjective assessment of penetrating execution

INTERNATIONAL JOURNAL OF RESEARCH IN MECHANICAL, MECHATRONICS AND AUTOMOBILE ENGINEERING(IJRMMAE)
ISSN: 2454-1435 (Print) | 2454-1443 (online)
Volume 6 Issue 4, January – March 2021 - www.ijrmmae.in – Pages 49-65

### 5.1 RAMAN ANALYSIS

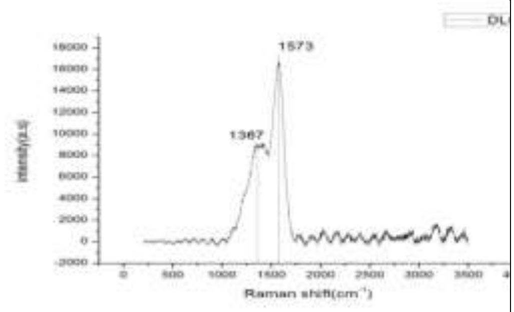


**Figure 4(a) Raman spectrum of DLC**

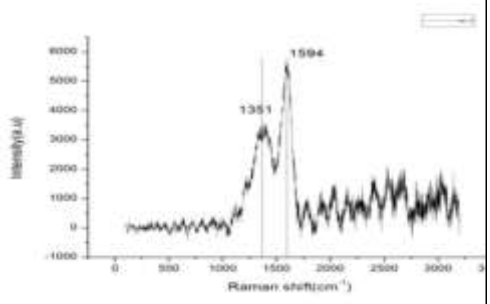


**Figure 4 (b) Raman spectrum of Ti-DLC**

Raman spectroscopy is the most effective way to acquire the nitty gritty holding designs of DLC films. Fig 4(a) and Fig 4 (b) shows the Raman spectra of as-saved DLC film and Ti doped DLC film separately. Both the Raman spectra show an expansive unbalanced top in the reach 1400-1700 cm_1, which is run of the mill of DLC films. The figure likewise shows a few clear contrasts between as-kept DLC film and Ti-doped DLC film. The Raman range of Ti-doped DLC film has the undeniable shoulder top at 1350 cm_1.this top demonstrative the Ti doped DLC structure.

### 5.2 SCANNING ELECTRON MICROSCOPE (SEM) ANALYSIS

SEM was utilized to concentrate on a superficial level morphology of the covered DLC and Ti-DLC In Fig 5a DLC picture has almost 1.2-1.8 micrometer breadth particles on the film surface which is as per AFM results. In Fig 5b DLC-Ti picture has nearly700-746 nm distance across particles on the film surface in this outcome likewise like the AFM result which concurs with the SEM perceptions. The doping of Ti on to DLC grid may a justification behind the shrinkage of grain size in the DLC network.

INTERNATIONAL JOURNAL OF RESEARCH IN MECHANICAL, MECHATRONICS AND AUTOMOBILE ENGINEERING(IJRMMAE)
ISSN: 2454-1435 (Print) | 2454-1443 (online)
Volume 6 Issue 4, January – March 2021 - www.ijrmmae.in – Pages 49-65

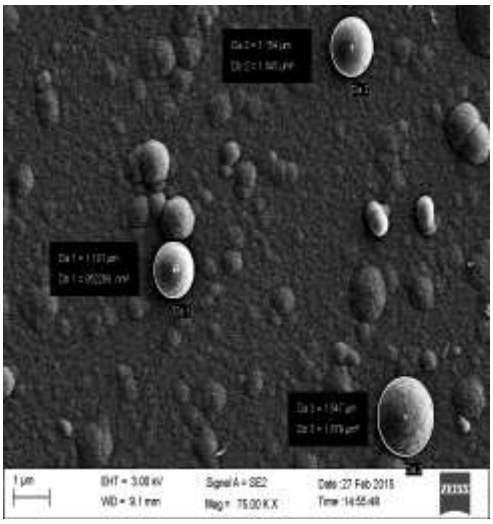

Figure 5(a) SEM image of DLC

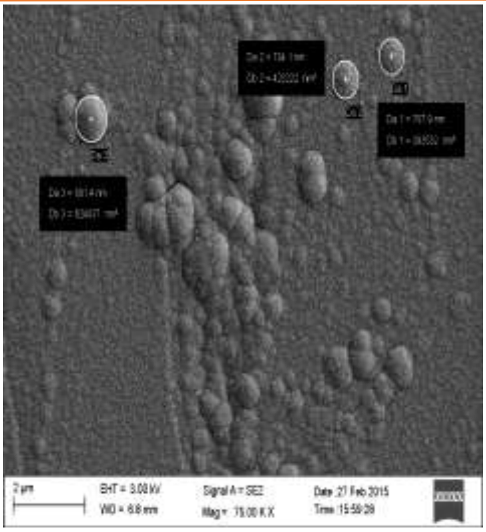

Figure 5(b) SEM image of Ti-DLC

### 5.3 COMPOSITION ANALYSIS BY EDAX

The principally EDAX is a semi quantitative strategy is utilized to figure out the creation of the examples. In Fig 5.5 and Fig 5.5b show the organization present in the DLC and Ti-DLC covered dainty film separately.

| | |
|---|---|
| 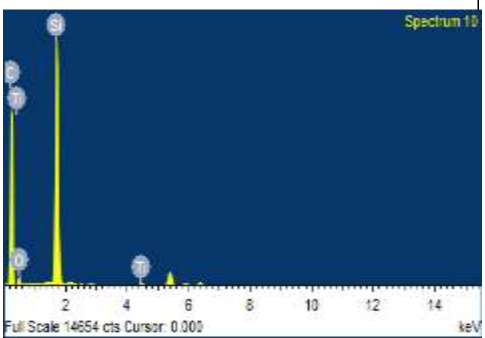  | 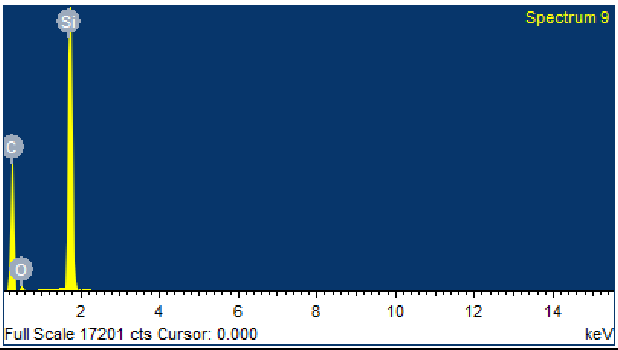  |
| Figure 6(a) elements presents on the film surface as- sputtered DLC thin film EDAX spectrum and composition | Figure 6(b) elements presents on the film surface as- sputtered DLC thin film EDAX spectrum and composition. |

INTERNATIONAL JOURNAL OF RESEARCH IN MECHANICAL, MECHATRONICS AND AUTOMOBILE ENGINEERING(IJRMMAE)
ISSN: 2454-1435 (Print) | 2454-1443 (online)
Volume 6 Issue 4, January – March 2021 - www.ijrmmae.in – Pages 49-65

| Element | Weight% | Atomic% |
|---|---|---|
| C K | 82.86 | 90.53 |
| O K | 4.13 | 3.39 |
| Si K | 13.01 | 6.08 |
| Totals | 100 | 100 |

| Element | Weight% | Atomic% |
|---|---|---|
| C K | 83.77 | 90.34 |
| O K | 6.36 | 5.15 |
| Si K | 9.64 | 4.45 |
| TiK | 0.22 | 0.06 |
| Total | 100 | 100 |

### 5.4 ATOMIC FORCE MICROSCOPY ANALYSIS (AFM)

The surface geology of 3D and geography picture of as-faltered DLC and DLC-Ti covered meager film are displayed in Fig 6(a) and Fig 6(b) ). Geology picture of the 25x25 micrometer region shows that a smooth surface is covered on the film surfaces. By the EDAX range these mass molecule pieces were viewed as equivalent to the objective structures thus these particles might be shot out from the objective material during faltering. Both the pictures show a smooth surface, yet with mass particles scattered on a superficial level. Surface unpleasantness boundaries like RMS harshness, and normal harshness were determined from the line profile across the imaged region.

The chart show that the unpleasantness profile of the DLC and Ti-DLC test separately. Both the normal harshness and RMS unpleasantness is established. Ti-DLC covered film unpleasantness is high contrast with the DLC covered slender film.

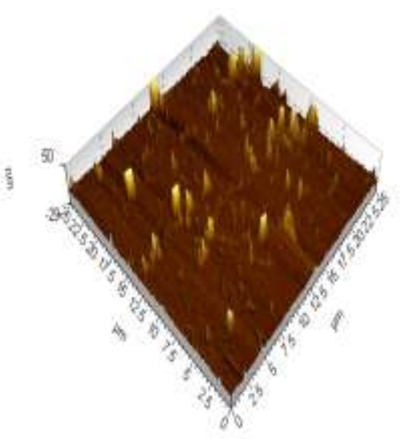

Figure 7(a) 3D image of DLC

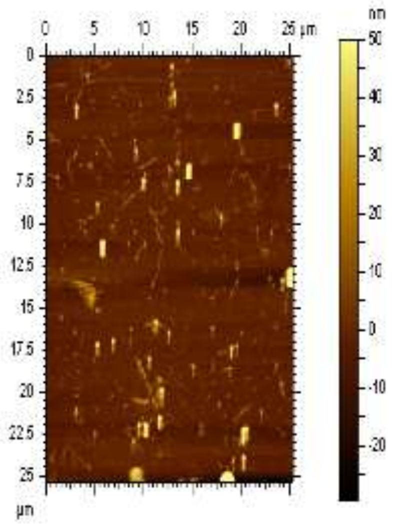


Figure 7(b) Topology image of DLC

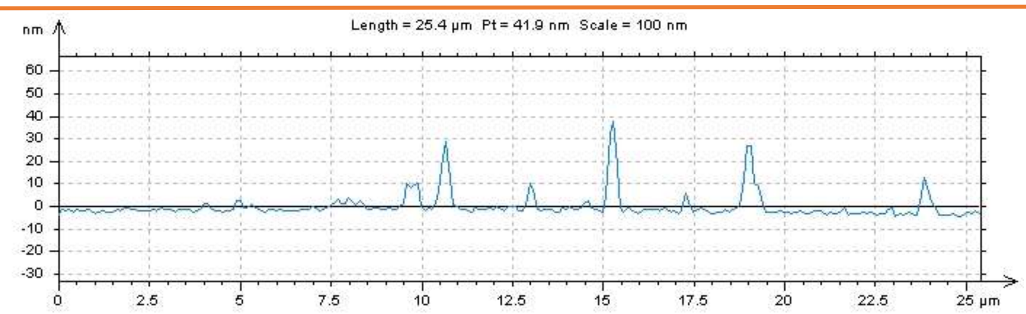


**Graph 5.1 Roughness graph for 25x25 micrometer area DLC thin film**

| Parameter | Values |
|---|---|
| Rp | 35.7 nm |
| Ra | 3.53 nm |
| Rq | 6.26 nm |

**Table 5.4 (a) as sputtered of DLC thin film**

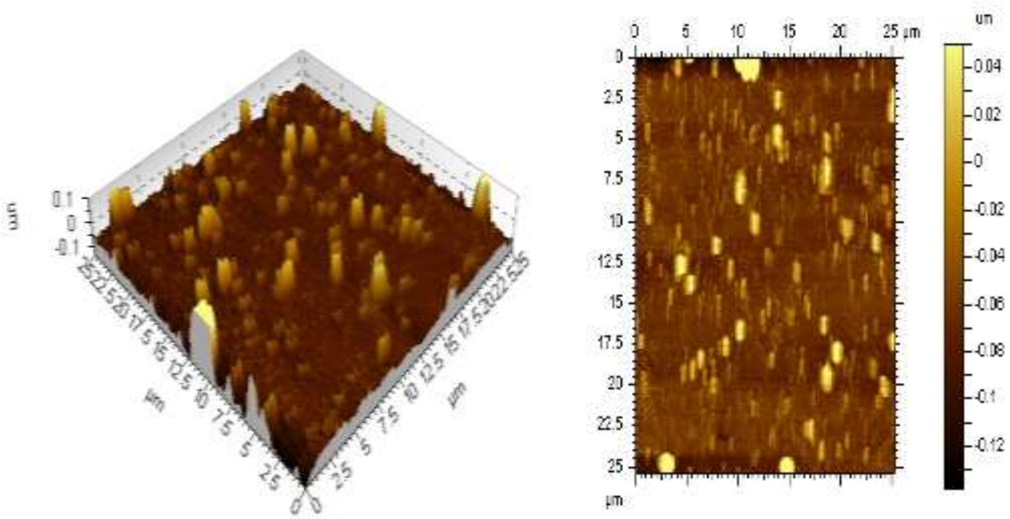

**Figure 8 (b) 3d image of DLC-Ti**

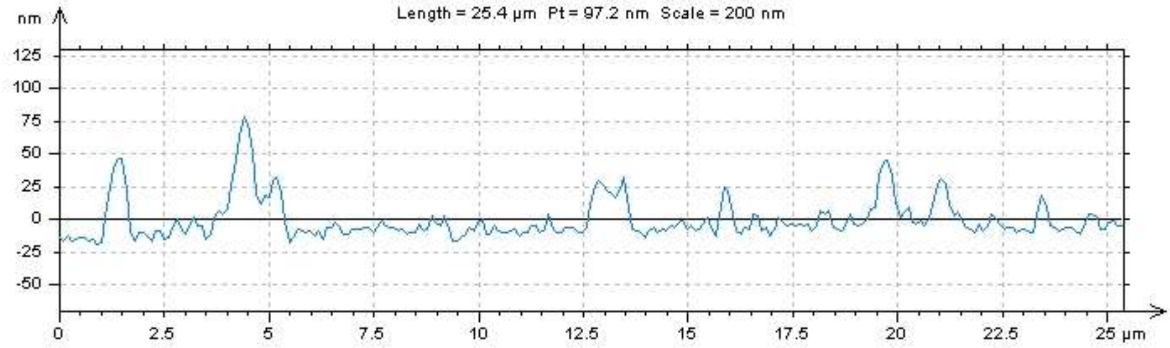


**Graph 5.1 Roughness graph for 25x25 micrometer area DLC-Ti thin film**

| Parameter | Values |
|---|---|
| Rp | 67.9 nm |
| Ra | 10 nm |
| Rq | 14.3 nm |

Table 5.4(b) as sputtered of DLC-Ti thin film

**5.5 Coefficient of friction;**

Block on ring wear analyzer was utilized to figure out the Coefficient Of Rubbing (COF) for DLC and Ti-DLC covered plate. In diagram 5.5(a) comparation between the DLC and Ti-DLC flimsy film. In this outcome Ti-DLC COF esteem is low contrast with the DLC.

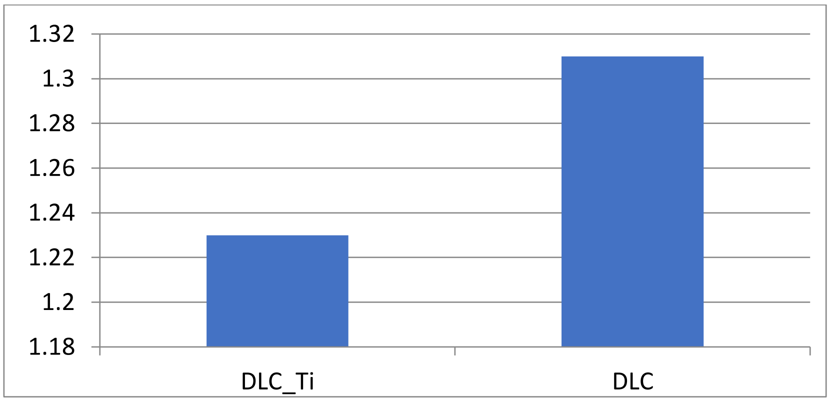


GRAPH 5.2 (a) Friction coefficient of DLC and Ti doped DLC

**5.6 QUALITATIVE EVALUATION OF DRILLING PERFORMANCE**

The subjective assessment of covered drill to bore the SS plate was finished to study the mechanical endure cutoff of DLC and Ti-DLC..The fig5.6a show the Fast I machine vision pictures when penetrating the substrates with DLC covered boring tools

ISSN: 2454-1435 (Print) | 2454-1443 (online)
Volume 6 Issue 4, January – March 2021 - www.ijrmmae.in – Pages 49-65

and Ti-DLC covered boring tools. In this comparation the Ti-DLC covered boring apparatus tip wear rate is low contrast with the DLC covered boring tools.

**Figure 9 (a) mission vission image of DLC coated drill bits**

**Figure 9(b) mission vission image of DLC-Ti coated drill bits**

Fig 6 shows the comparation for covered and un covered boring tools execution. In this comparision precious stone like carbon and Ti doped jewel like carbon covered boring apparatus activity execution is better contrast with the uncoated bores execution.

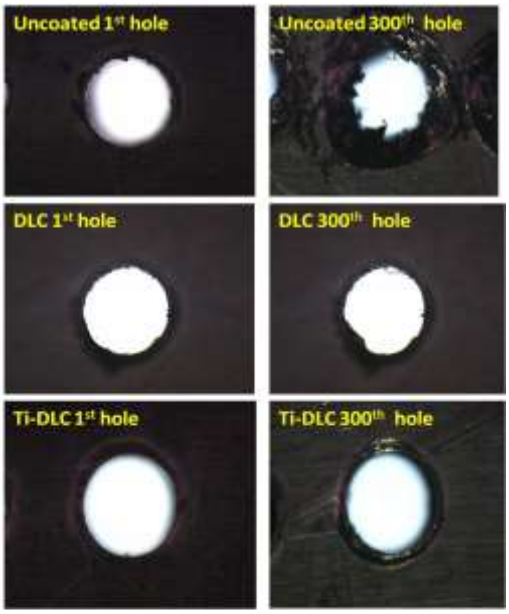


Fig 10 (a)first opening for uncoated penetrated (b)300th opening for uncoated bored (c)first opening for dlc covered penetrated (d)300th opening for dlc covered bored (e)first opening for dlc-ti covered bored (f) 300th opening for DLC-Ti covered bored.

## REFERENCE


1) S. Brown, J. Lengaigne, N. Sharifi, M. Pugh, C. Moreau, A. Dolatabadi, L. Martinu, J.E. Klemberg-Sapieha, 2020. Durability of superhydrophobic duplex coating systems for aerospace applications. Surf. Coat. Technol. 401, 126249.
2) E.R. Sivakumar, P.S. Kumar, M. Sreenivasan, R. Krishna, Experimental investigation of H-DLC coated exhaust valve characteristics of a diesel engine, Mater. Today Proc. 33 (2020) 678-681.
3) https://www.sciencedirect.com/science/article/abs/pii/S0165993602012086
4) T. Hasebe, A. Hotta, H. Kodama, A. Kamijo, Recent advances in diamond-like carbon films in the medical and food packing fields, N. Diam, Front. Carbon Technol. 17 (2007) 263- 279. Page 18 of 33
5) H. Ferhati, F. Djeffal, N. Boubiche, F.L. Normand, An efficient ITO-free transparent electrode based on diamond-like carbon with an engineered intermediate metallic thin-film, Sol. Energy 196 (2020) 327-335.
6) M.S. Kabir, Z. Zhou, Z. Xie, P. Munroe, Designing multilayer diamond like carbon coatings for improved mechanical properties, J. Mater. Sci. Technol. 65 (2021) 108-117.
7) X. Rao, J. Yang, Z. Chen, Y. Yuan, Q. Chen, X. Feng, L. Qin, Y. Zhang, Tuning C–C sp2 /sp3 ratio of DLC films in FCVA system for biomedical application, Bioact. Mater. 5 (2020) 192-200.
8) K. Komori, T. Nagataki, Friction Behavior of Diamond-Like Carbon Coated Ball Joint: Approach to Improving Vehicle Handling and Ride-Comfort, SAE Int. J. Passeng. Cars - Mech. Syst. 8 (2015) 638-646.
9) https://www.sciencedirect.com/science/article/pii/S0268401223000233.
10) W. Yu, J. Wang, W. Huang, L. Cui, L. Wang, Improving high temperature tribological performances of Si doped diamond-like carbon by using W interlayer, Tribol. Int. 146 (2020) 106241.
11) https://www.researchgate.net/publication/225477777_Characterization_of_DC_magnetron_sputtered_diamond-like_carbon_DLC_nano_coating
12) https://www.sciencedirect.com/topics/chemistry/vibrational-method
13) https://www.sciencedirect.com/topics/materials-science/diamond-like-carbon-coating
14) https://www.sciencedirect.com/science/article/abs/pii/S0925963520305495.